DESIGN AND ANALYSIS OF RADOMES FOR MICROSTRIP PATCH ANTENNA AT 6 GHZ

Using Ansys HFSS

Aleena Ann Jacob

Catholicate College, MG University

Krittika Summer Project • IIT Bombay

July 2025

DESIGN AND ANALYSIS OF RADOMES FOR MICROSTRIP PATCH ANTENNA AT 6GHZ

by

ALEENA ANN JACOB

A thesis submitted as part of
Krittika Summer Project
IIT Bombay

Catholicate College
Affiliated under Mahatma Gandhi University
Pathanamthitta
24/07/2025

Abstract

Radome-integrated antenna systems are increasingly employed across high-frequency applications, where environmental robustness must be balanced against electromagnetic performance. In this study, a planar microstrip patch antenna operating at 6 GHz is enclosed within a flat PMMA-based dielectric radome and analyzed using full-wave simulation tools. A detailed modeling approach is adopted to investigate the influence of radome material, thickness, and placement on key antenna parameters such as return loss, gain, and radiation efficiency. Simulation results demonstrate that while the radome introduces marginal beam broadening and a slight peak shift in gain direction, overall impedance stability.

The findings confirm that appropriate radome design can protect antenna integrity with minimal distortion, supporting its viability in compact, high-frequency sensing platforms.

Acknowledgements

I would like to extend my sincere gratitude to Mr. Arjun Ghosh for his exceptional guidance and unwavering support throughout the course of this project. His insights and mentorship were instrumental to its success.

I am deeply thankful to Krittika, the astronomy club of IIT Bombay, for providing this invaluable research opportunity and equipping us with the resources needed to bring the study to life.

My heartfelt appreciation goes to my teammates Sandipan, Dileep, Anvit, and Manohara for their relentless dedication, constructive collaboration, and strong team spirit. I am profoundly grateful to Sandipan, who selflessly devoted his time and energy to support me, often going above and beyond to deliver thoughtful solutions and fruitful results.A special mention to Anvit, whose constant help during challenging phases made a significant difference

I also wish to thank our project facilitator, Ms. Aditi Singh, for her steady coordination and helpful guidance throughout our journey.

Contents

List of Figures

Acronyms

PMMA Polymethyl Methacrylate

CAD Computer-aided Design

RF Radio Frequency

PTFE Polytetrafluroethylene

EM Electromagnetic

Chapter 1

Introduction

Antennas play a crucial role in enabling the transmission and reception of electromagnetic waves, serving as the gateway between electronic systems and the wireless world around us. They function by converting electrical signals into electromagnetic radiation for transmission, and vice versa for reception. From satellite communication to mobile phones, and from television broadcasting to radar systems, antennas are foundational components in virtually every wireless technology. Their design determines key performance characteristics, including radiation pattern, gain, bandwidth, and polarization, all of which influence how effectively they communicate across distances and directions.

As modern systems demand increasingly compact and integrated solutions, microstrip patch antennas have emerged as an essential innovation. A microstrip patch antenna is a type of low-profile, planar antenna widely used in modern wireless communication systems due to its compact size, ease of fabrication, and compatibility with integrated circuits. These antennas feature a metallic patch mounted on a dielectric substrate, with a ground plane beneath. The patch can take various shapes: rectangular, circular, triangular, though rectangular is most common due to its simplicity and predictable performance.

These antennas operate primarily at microwave frequencies (typically above 1 GHz) and are favoured for applications such as satellite communication, mobile devices, GPS, and radar systems. Their popularity stems from their lightweight structure, low cost, and ability to support both linear and circular polarization. However, microstrip patch antennas typically suffer from narrow bandwidth and lower efficiency compared to other antenna types, which can be mitigated through design techniques like stacking, slotting, or using parasitic elements.

The radiation mechanism is based on fringing fields at the edges of the patch, and the antenna behaves like a resonant cavity with radiating slots. Feeding methods include microstrip line, coaxial probe, aperture coupling, and proximity coupling, each offering trade-offs in terms of bandwidth, complexity, and radiation characteristics.

Due to their versatility and adaptability, microstrip patch antennas continue to be a cornerstone in antenna engineering, especially in compact and conformal systems.

Chapter 2

Microstrip Patch Antenna

2.1 Structure of Microstrip Patch Antenna

Patch Antenna or Microstrip Antenna comprises a patch, substrate and ground plane. These antennas are used in various fields of radio astronomy. The structure of a patch antenna includes the following:

2.1.1 Radiating Patch

A thin metallic conductor (often copper or gold) of various shapes (rectangular, circular, elliptical, triangular, etc.) on one side of a dielectric substrate. When fed with radio frequency (RF) energy, the currents on the patch generate electromagnetic waves that radiate into space. The dimensions of the patch are crucial as they determine the antenna's resonant frequency.

2.1.2 Dielectric substrate

An insulating material that separates the radiating patch from the ground plane. Common materials include FR4, Rogers, and Duroid, each with different dielectric constants. The thickness of the substrate is typically a small fraction of the wavelength (around 0.03λ to 0.05λ). This dielectric had multiple uses:

- It mechanically supports the radiating patch and the microstrip feed line.
- It maintains a precise separation between the patch and the ground plane, which is best for the antenna's electrical performance (impedance, bandwidth).
- The dielectric constant of the substrate affects the effective waves propagating underneath the patch.

2.1.3 Ground plane

A continuous metallic layer on the opposite side of the dielectric substrate, forming a stable reference point. It helps to confine the electromagnetic fields between the patch and the ground plane, contributing to the resonant behaviour.

2.1.4 Microstrip feed line

In an edge-fed configuration, a thin metallic strip (also copper) extends directly from the edge of the radiating patch to connect with the RF source
The figure here represents the top view of the microstrip antenna:

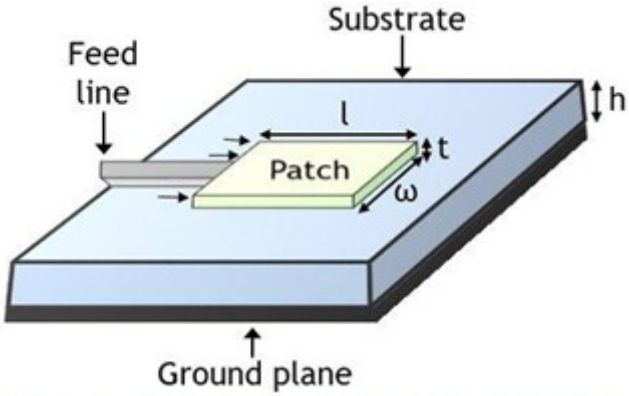

Figure 2.1: Top-view of Microstrip Patch Antenna (Electronicsdesk.com)

2.2 Feeding techniques for Microstrip Patch Antenna

Despite certain limitations such as narrow bandwidth and moderate efficiency, microstrip patch antennas offer sufficient performance for many applications. Design enhancements, such as array configurations, stacked patches, and varied feed techniques, help mitigate these challenges. Rather than connecting the feed line at the very edge of the patch, an inset feed introduces the feed line at a specific distance (the "inset") from the edge. The microstrip feed line is notched into the radiating patch by a specific distance called an inset. This creates a small gap or slot between the main body of the patch and the portion of the patch that's connected to the feed line.

2.2.1 Inset feeding

When a microstrip patch antenna is designed to resonate at a particular frequency, the input impedance (the impedance seen looking into the antenna from the feed point) varies significantly across its surface. In electrical circuits, impedance (Z) is a measure of the opposition that a circuit presents to a current when a voltage is applied. At the very edges of a rectangular patch, particularly the radiating edges, the input impedance is generally very high (often hundreds of ohms). As you move inward from the edge along the length of the patch, the input impedance progressively decreases. Inset-feeding allows you to "tap into" the patch at a specific point where its input impedance is 50 ohms (or very close to it) at the resonant frequency. By doing this, you create an effective impedance match, ensuring that almost all the RF power delivered by the feed line is radiated efficiently by the antenna. So, in order to reduce the S11 loss, we can take a specific inset distance into the patch and apply the RF energy with the help of this inset-feeding technique which will

eventually lead to lower return loss, better power transfer, and higher radiation efficiency and also reducing the need for additional matching circuits.

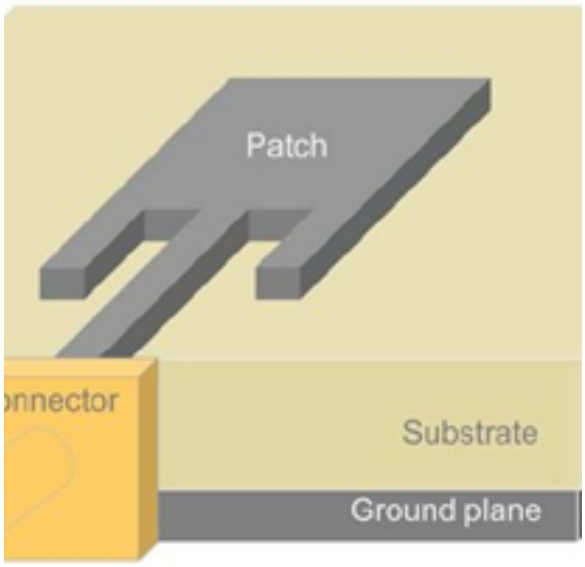

Figure 2.2: Top and side view of inset-feeding microstrip patch antenna [3]

Chapter 3

Inset-fed Microstrip Patch Antenna at 6GHz

3.1 Design

While we design a microstrip patch antenna, we have to consider some dimensions and parameters corresponding to the patch, substrate and ground plane. Before that, let us consider that the substrate we took is FR4, whose dielectric constant is approximately 4.2 (a commonly accepted value for FR4 at 6 GHz, though variability exists) and the standard thickness for this substrate is 1.6 mm. Now, the equations that needs to be considered while designing are as follows:

3.1.1 Width of the patch (W)

$$W = \frac{c}{2f_r}\sqrt{\frac{2}{\varepsilon_r + 1}} \tag{3.1}$$

Let's plug in the values and calculate the dimensions. Given Parameters:

- Resonant Frequency (f_r): 6 GHz = 6×10^9 Hz
- Speed of Light (c): 3×10^8 m/s
- Substrate height $h = 1.6$ mm = 1.6×10^{-3} m
- Dielectric constant $\varepsilon_r = 4.4$

$$W = \frac{c}{2f_r}\sqrt{\frac{2}{\varepsilon_r + 1}} \tag{3.2}$$

$$= \frac{3 \times 10^8}{2 \times 6 \times 10^9}\sqrt{\frac{2}{4.4 + 1}} \tag{3.3}$$

$$= 0.025 \times 0.60858 \tag{3.4}$$

$$= 0.01521 \text{ m} \tag{3.5}$$

$$= 15.215 \text{ mm} \tag{3.6}$$

3.1.2 Effective Dielectric Constant (ε_{eff})

This accounts for the electric field lines extending partially into the air above the substrate.

$$\varepsilon_{\text{eff}} = \frac{\varepsilon_r + 1}{2} + \frac{\varepsilon_r - 1}{2}\left(1 + 12 \cdot \frac{h}{W}\right)^{-1/2} \tag{3.7}$$

Plugging in the values:

$$\varepsilon_{\text{eff}} = \frac{4.4 + 1}{2} + \frac{4.4 - 1}{2}\left(1 + 12 \cdot \frac{1.6 \times 10^{-3}}{15.215 \times 10^{-3}}\right)^{-1/2} \tag{3.8}$$

$$\varepsilon_{\text{eff}} = 2.7 + 1.7 \cdot (2.26191)^{-1/2} \tag{3.9}$$

$$\varepsilon_{\text{eff}} = 2.7 + 1.13034 \tag{3.10}$$

$$\varepsilon_{\text{eff}} = 3.830 \tag{3.11}$$

3.1.3 Effective Length (L_{eff})

This is the theoretical length of the patch in the presence of the effective dielectric constant.

$$L_{\text{eff}} = \frac{c}{2f_r\sqrt{\varepsilon_{\text{eff}}}} \tag{3.12}$$

$$L_{\text{eff}} = \frac{3 \times 10^8}{2 \times 6 \times 10^9 \cdot \sqrt{3.830}} \tag{3.13}$$

$$L_{\text{eff}} = \frac{1}{40 \cdot 1.95713} \tag{3.14}$$

$$L_{\text{eff}} = 0.01277440 \text{ m} \tag{3.15}$$

$$L_{\text{eff}} = 12.774 \text{ mm} \tag{3.16}$$

3.1.4 Length Extension (ΔL)

In a purely theoretical sense, if all the electric and magnetic fields were perfectly confined between the patch and the ground plane, the antenna would resonate when its physical length (L) was exactly half of the effective wavelength (λ eff /2) in the substrate. But in practice, at the edges of the patch, the electric field lines do not abruptly stop. Instead, they fringe out from the patch into the surrounding air and then curve back down to terminate on the ground plane. The length extension, ΔL term in the equations is precisely to account for these fringing fields.

$$\Delta L = 0.412h \cdot \frac{(\varepsilon_{\text{eff}} + 0.3)\left(\frac{W}{h} + 0.264\right)}{(\varepsilon_{\text{eff}} - 0.258)\left(\frac{W}{h} + 0.8\right)} \tag{3.17}$$

$$\Delta L = 0.412 \cdot 1.6 \times 10^{-3} \cdot \frac{(3.830 + 0.3)\left(\frac{15.215}{1.6} + 0.264\right)}{(3.830 - 0.258)\left(\frac{15.215}{1.6} + 0.8\right)} \tag{3.18}$$

$$\Delta L = 0.412 \cdot 1.6 \times 10^{-3} \cdot \frac{4.13 \cdot (9.509 + 0.264)}{3.572 \cdot (9.509 + 0.8)} \tag{3.19}$$

$$\Delta L = 0.412 \cdot 1.6 \times 10^{-3} \cdot \frac{4.13 \cdot 9.773}{3.572 \cdot 10.309} \tag{3.20}$$

$$\Delta L = 0.412 \cdot 1.6 \times 10^{-3} \cdot \frac{40.38749}{36.833548} \tag{3.21}$$

$$\Delta L = 0.412 \cdot 1.6 \times 10^{-3} \cdot 1.0963 \tag{3.22}$$

$$\Delta L = 0.00072341 \text{ m} \tag{3.23}$$

$$\Delta L = 0.723 \text{ mm} \tag{3.24}$$

3.1.5 Actual Length(L)

This is the physical length of the patch.

$$L = L_{\text{eff}} - 2\Delta L \tag{3.25}$$

$$= 12.774 \text{ mm} - 2 \times 0.723 \text{ mm} \tag{3.26}$$

$$= 12.774 - 1.446 \tag{3.27}$$

$$= 11.329 \text{ mm} \tag{3.28}$$

3.1.6 Input Impedance (Z_{in})

The input impedance of a microstrip patch antenna is the electrical impedance seen by the feed line at the point where it connects to the antenna.

$$Z_{\text{in}} = 90 \cdot \left(\frac{\varepsilon_r^2}{\varepsilon_r - 1}\right)\left(\frac{L}{W}\right)^2 \tag{3.29}$$

$$Z_{\text{in}} = 90 \cdot \left(\frac{4.4^2}{4.4 - 1}\right)\left(\frac{11.329}{15.215}\right)^2 \tag{3.30}$$

$$Z_{\text{in}} = 90 \cdot \left(\frac{19.36}{3.4}\right) \cdot (0.7441)^2 \tag{3.31}$$

$$Z_{\text{in}} = 90 \cdot 5.6941 \cdot 0.5537 \tag{3.32}$$

$$Z_{\text{in}} = 284.124\ \Omega \tag{3.33}$$

3.1.7 Transmission Line Width (W_0)

The transmission line width refers to the physical width of the microstrip line (feed line) used to carry RF signals from the source to the patch antenna.

$$W_0 = 2.377 \text{ mm} \tag{3.34}$$

3.1.8 Inset spacing (S)

Inset spacing is the distance from the edge of the patch to the feed point along the patch's centerline. It is used in inset-fed microstrip patch antennas to control the input

impedance and achieve impedance matching (typically to 50 Ω.

$$S = \frac{1}{2}W_0 \tag{3.35}$$
$$= 0.5 \times 2.377 \tag{3.36}$$
$$= 1.685 \text{ mm} \tag{3.37}$$

3.1.9 Substrate and Ground plane dimensions- The 6h rule

To reduce edge effects and enhance radiation performance, the substrate and ground plane dimensions are empirically extended by a margin of 3h on all sides, resulting in a total increase of 6h in both the width and length of the patch.

$$W_{\text{sub}} = w + 6h \tag{3.38}$$

where:

$$L_{\text{sub}} = l + 6h \tag{3.39}$$

w= 15.215 mm (Patch width)

h = 1.6 mm (Substrate height)

l = 11.329 mm (Patch length)

$$W_{\text{sub}} = 15.215 + 6 \times 1.6 \tag{3.40}$$
$$= 24.815 \text{ mm} \tag{3.41}$$
$$L_{\text{sub}} = 11.329 + 6 \times 1.6 \tag{3.42}$$

and

$$= 20.129 \text{ mm} \tag{3.43}$$

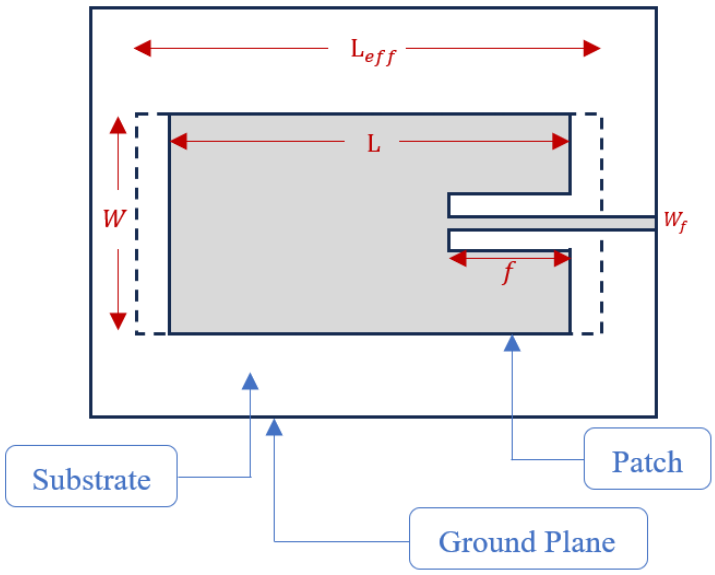

Figure 3.1: Dimensions of Microstrip Patch Antenna

3.2 CAD modelling

The design of the microstrip patch antenna operating at 6 GHz was implemented using Ansys HFSS, leveraging a detailed set of analytical calculations to ensure optimal performance. Designed for a 6 GHz resonant frequency on an FR4 substrate, the

antenna's characteristics were investigated in free-space operation, as well as when integrated with flat and spherical radome geometries. The antenna is designed under a layered construction: a ground plane, a dielectric substrate, the radiating patch, and an inset-fed transmission line. The dimensions for all components were derived from established design parameters.

3.2.1 Ground plane

A 24.815 mm × 20.129 mm rectangle was sketched on the XY-plane to define the ground plane. This sketch was then extruded to a thickness of 0.0035 mm, representing the copper ground layer.

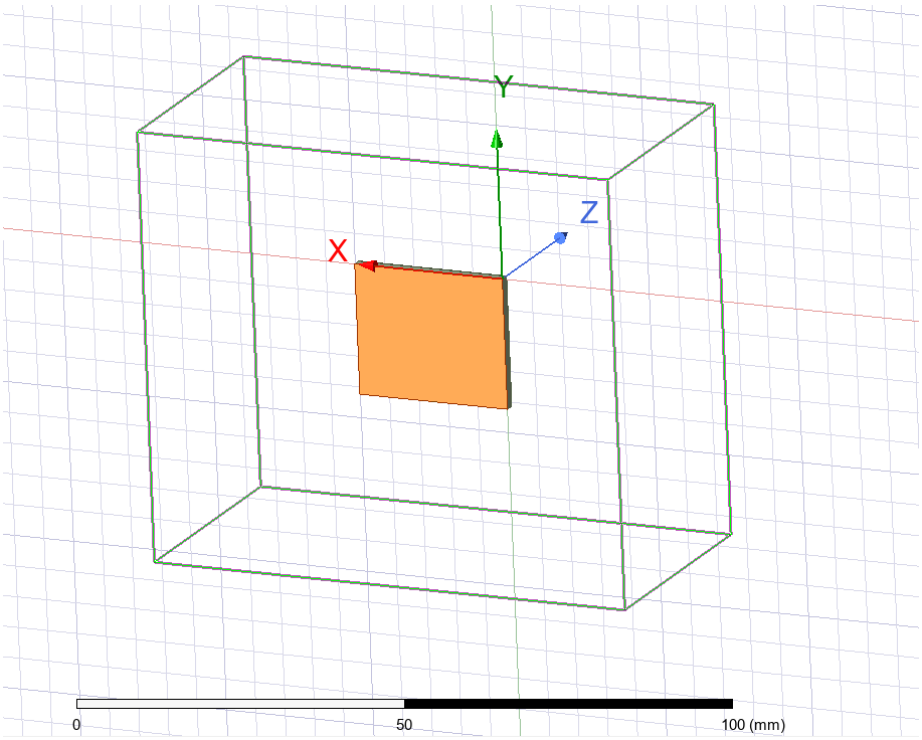

Figure 3.2: Ground plane in the CAD model

3.2.2 Substrate

Immediately above the ground plane, the dielectric substrate was defined. A rectangular sketch, identical in dimensions to the ground plane (24.815 mm × 20.129 mm), was created. This substrate layer was given a thickness (height) of 1.6 mm, and its material properties were set to FR4 epoxy, a common dielectric for microwave applications.

3.2.3 Patch

Serving as the primary radiating element, the patch was modeled as a rectangle positioned on the top surface of the dielectric substrate. This copper layer featured precise dimensions of 15.215 mm × 11.329 mm and was subsequently extruded to a standard thickness of 0.0035 mm to represent the conductive material.

3.2.4 Feedline

To facilitate impedance matching, an inset cut was strategically introduced along one of the longer (non-radiating) sides of the patch. The inset depth was precisely set to 2.9 mm to ensure optimal impedance transformation. The inset width was specified as 1.5 mm, intentionally made slightly narrower than the connecting feed line. Finally, a microstrip feed line with a width of 2.377 mm was designed, then extruded to a thickness of 0.0035 mm, and meticulously aligned centrally within the inset to establish the electrical connection to the radiating patch.

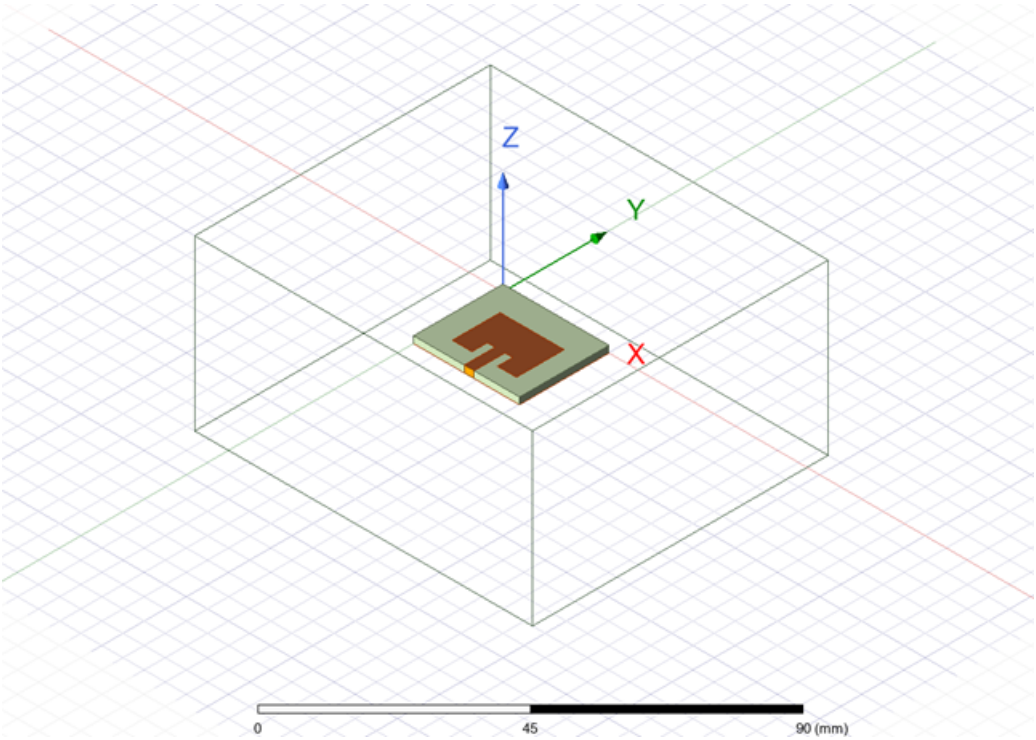

Figure 3.3: Microstrip patch antenna CAD model designed in ANSYS HFSS

3.3 Simulations and optimisations

Validation and performance optimization of the antenna design were achieved through a detailed electromagnetic simulation executed in ANSYS HFSS. This simulation primarily aimed to characterize the antenna's operational behavior at 6 GHz. The CAD model setup in ANSYS was analyzed by defining the variables and then by doing parametric sweep.

3.3.1 Simulation Setup Overview

Material Definition

1. Copper was selected as the conductive material for both the radiating patch and ground plane due to its excellent electrical conductivity.

2. The substrate was defined as FR4 Epoxy, characterized by a relative permittivity $\varepsilon_r = 4.4$ and a loss tangent of 0.02.

Excitation Configuration

3. A rectangular interface was created at the junction of the feed line, substrate, and ground plane to define the excitation region.

4. This region was assigned a Lumped Port with a reference impedance of $50\,\Omega$, enabling standard impedance matching.

Boundary Conditions

5. A radiation boundary box was constructed around the antenna, positioned atleast $\lambda/4$ distance from the antenna edges, ensuring minimal field reflection.

6. Boundary assignments included:

   - The patch and ground plane as Perfect Electric Conductors (PEC).
   - The external faces of the radiation box as Radiation boundaries to allow wave propagation into free space.

Solution Parameters

7. The operating frequency was set at 6 GHz, with a maximum of 20 adaptive passes to ensure convergence.

8. A frequency sweep was defined from 4.5 GHz to 7.5 GHz, generating 401 data points. Additionally, angular sweep settings were applied:

   - Azimuthal angle θ ranged from 0° to 360° in 2° increments.

Parametric Analysis

9. A parametric sweep was performed on the inset depth, varying it from 2 mm to 4 mm in increments of 0.4 mm. This enabled analysis of impedance variation to determine the optimal inset depth for minimizing reflection coefficient $|S_{11}|$.

Far-Field Configuration

10. A Far-Field Infinite Sphere setup was configured to analyze radiation characteristics:

    - Elevation angle ϕ ranged from 0° to 90°.
    - Azimuthal angle θ spanned 0° to 360°, both sampled at appropriate intervals.

3.3.2 Result Extraction

The simulation yielded key performance indicators:

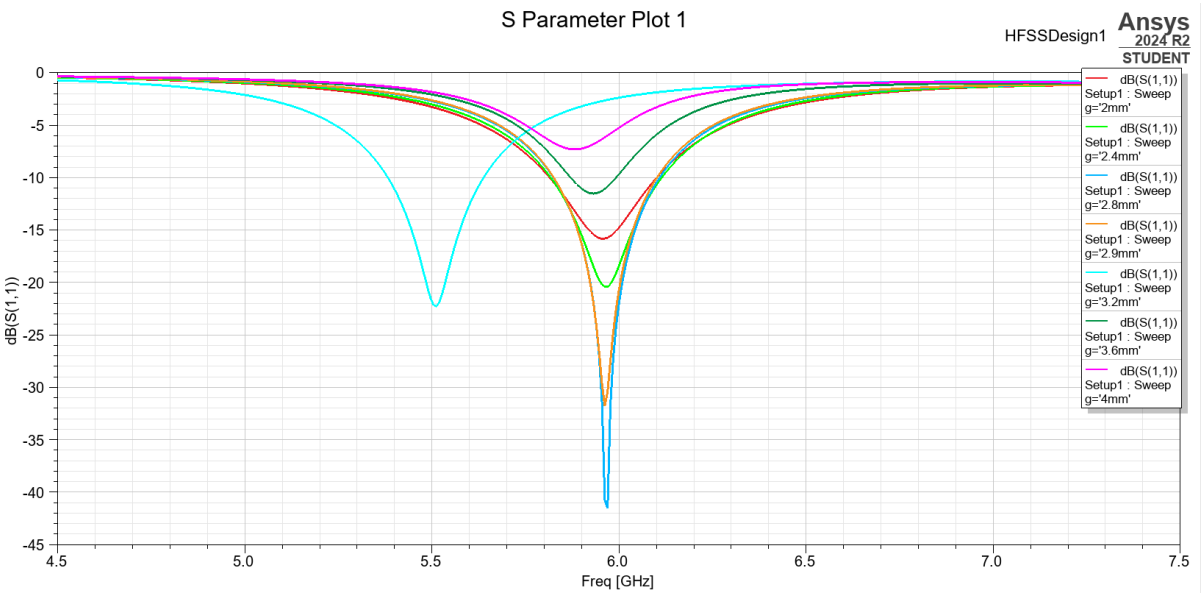

Figure 3.4: Return loss plot from parametric sweep

- **2D radiation plots for directional characteristics.**

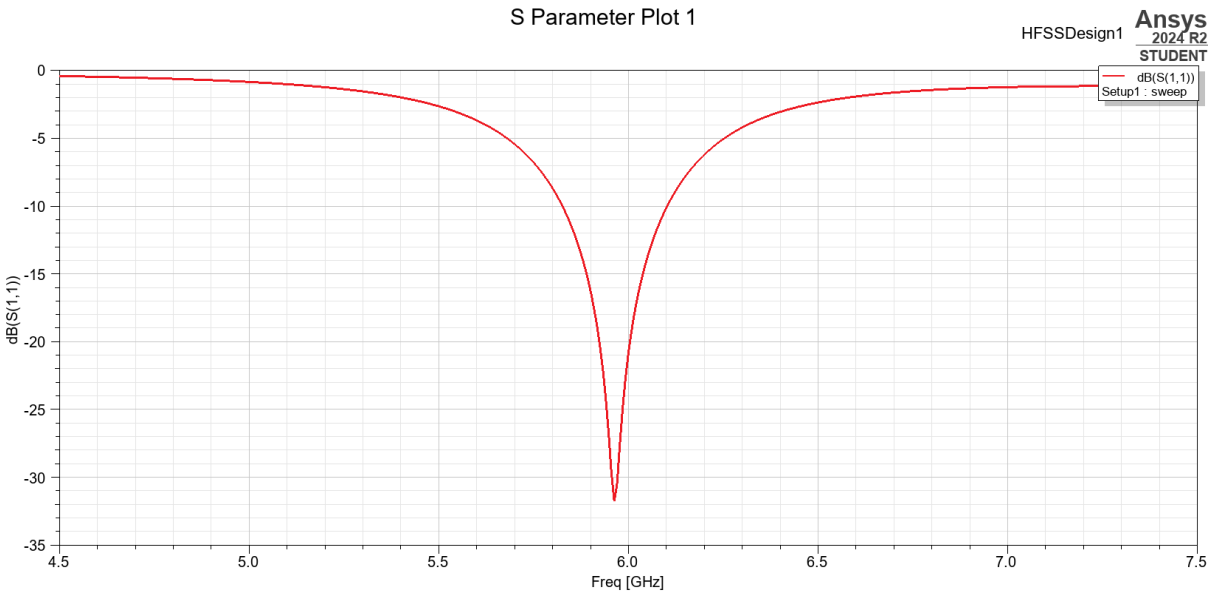

Figure 3.5: S11 parameter plot

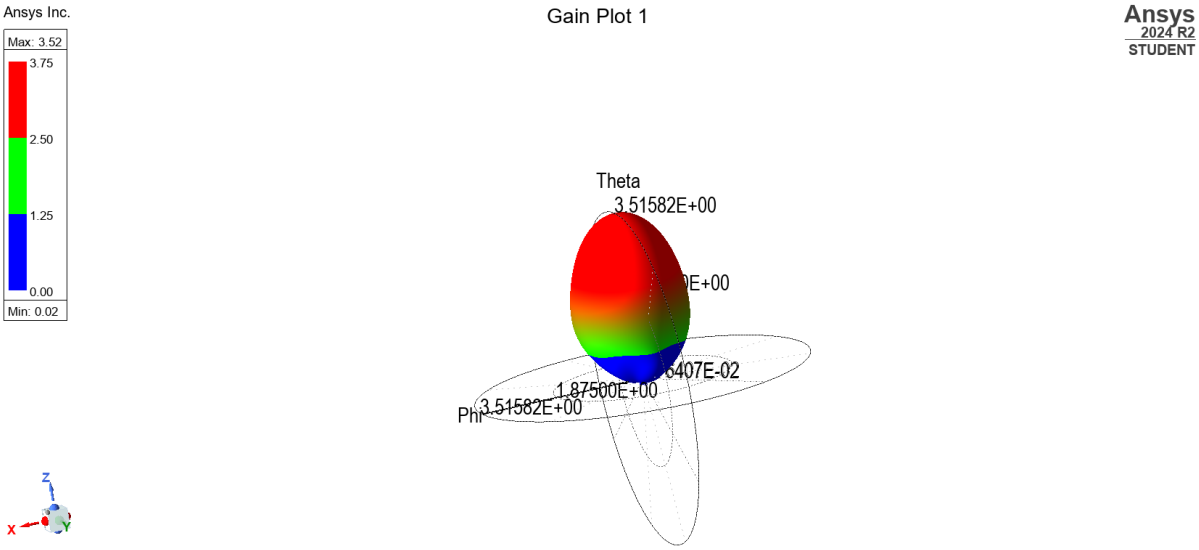

Figure 3.6: 3D polar total gain plot for H and E planes

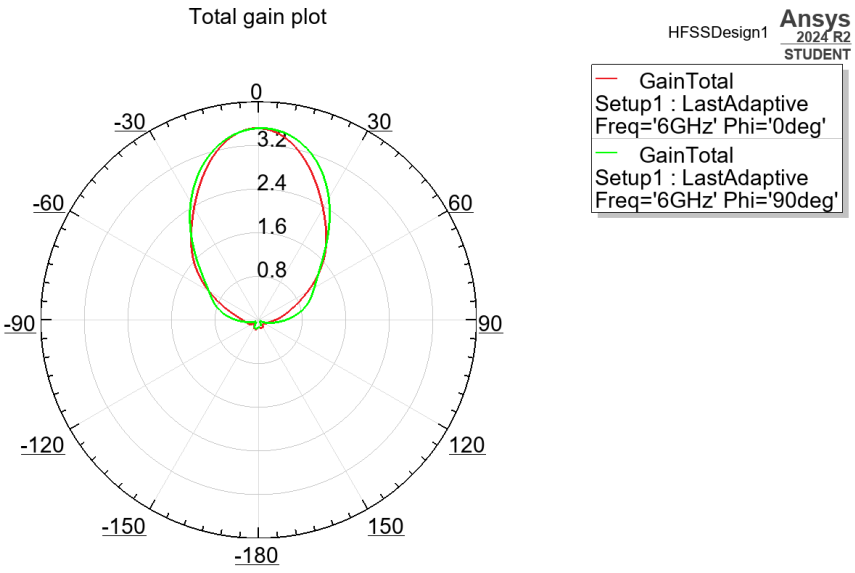

Figure 3.7: E and H plane gain total plots

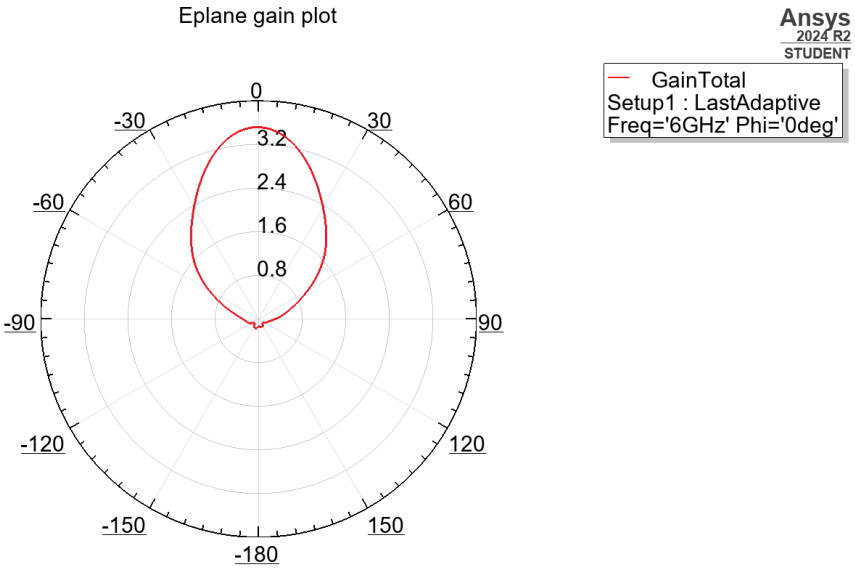

Figure 3.8: 2D gain plot for E plane

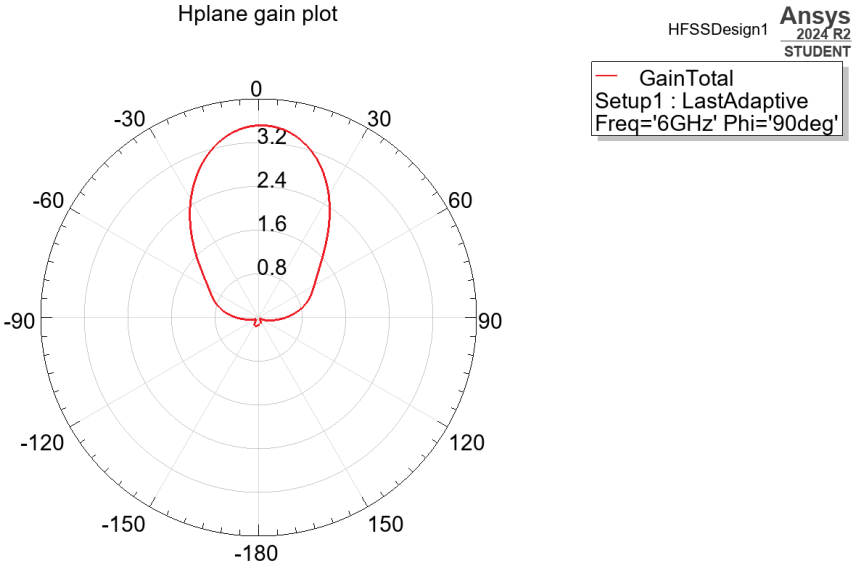

Figure 3.9: 2D gain plot for H plane

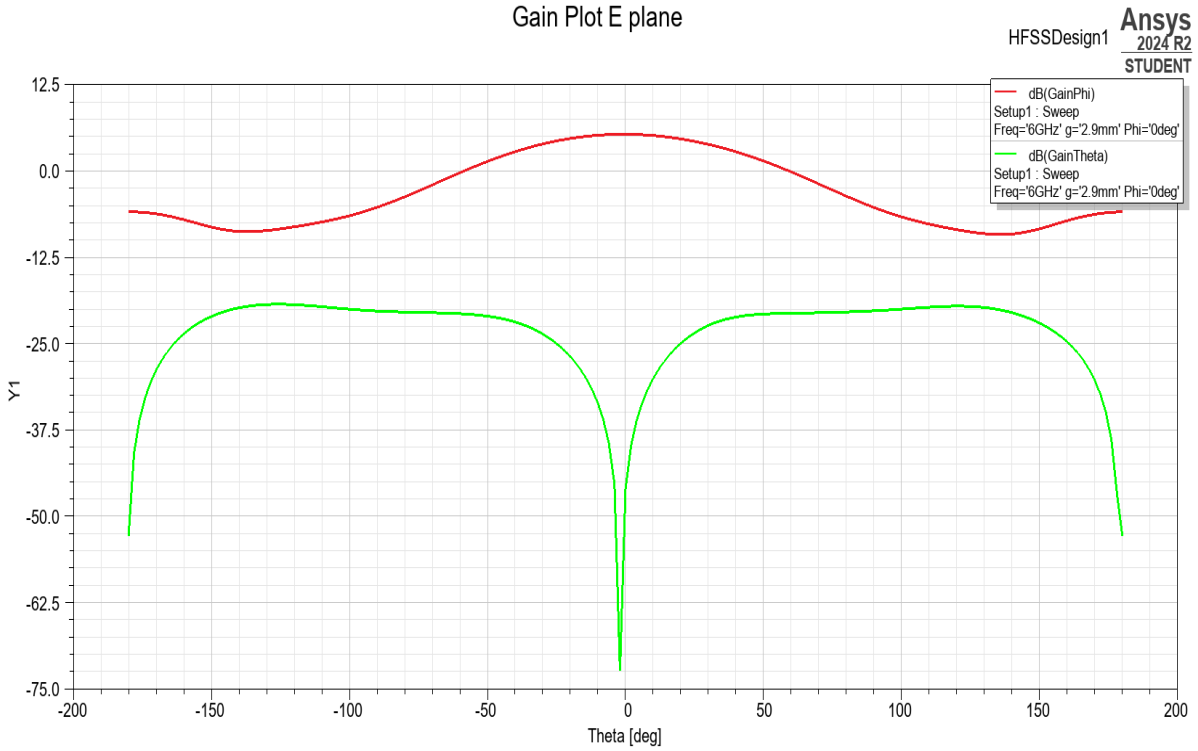

Figure 3.10: Cross polarized gain plot (gain phi and gain theta) for E plane

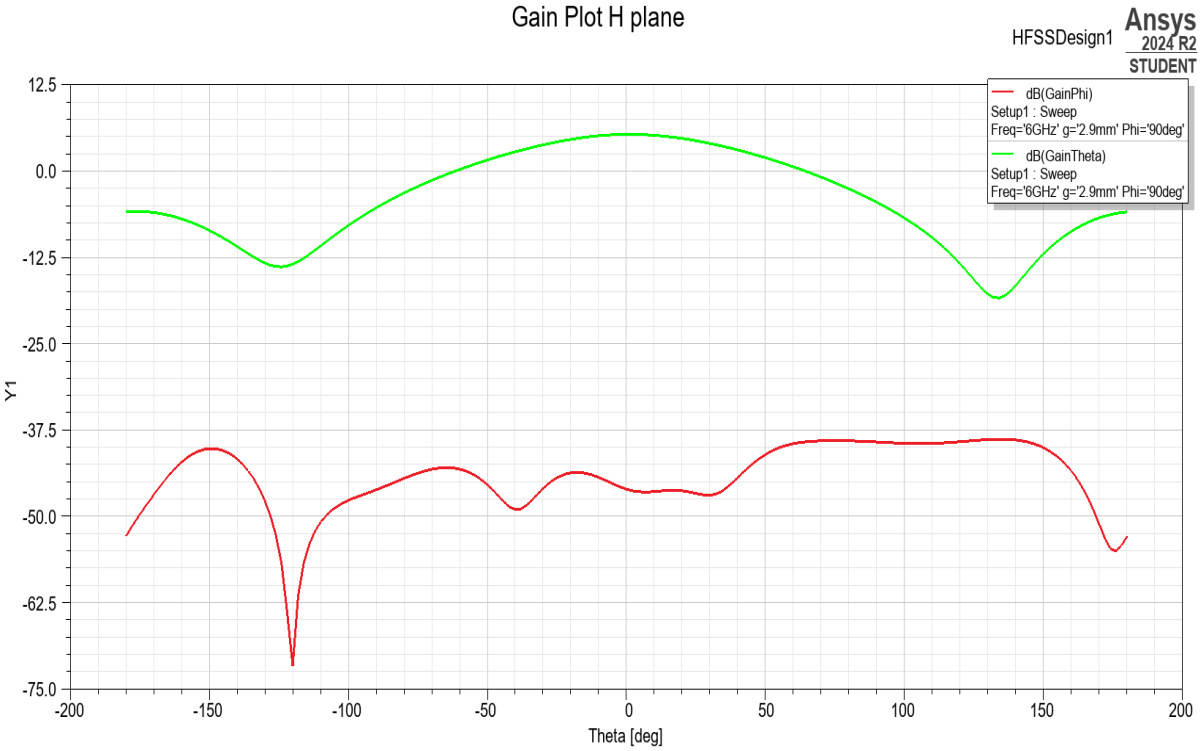

Figure 3.11: 2D cross polarized gain plot (gain phi and gain theta) for H plane

Chapter 4

Radome

4.1 What are Radomes?

A radome is a specialized enclosure designed to shield mmWave radar antennas and electronics from environmental hazards such as moisture, sunlight, dust, and wind. Although offering mechanical protection and weatherproofing, the radome maintains electromagnetic transparency, minimally attenuating the transmitted and received signals, allowing seamless propagation of radio waves. For optimal performance, the radome material must exhibit low dielectric loss and minimal signal distortion.

In certain designs, radomes function as dielectric lenses, intentionally modifying the antenna's beam direction or shape. These types require co-design with the antenna system using electromagnetic simulation tools, ensuring the altered radiation characteristics meet application-specific field-of-view or gain requirements.

Radomes come in a variety of geometries tailored to system constraints and performance goals. Common forms include planar, spherical, and geodesic domes, each influencing the antenna's radiation pattern and effective range differently. The choice of shape plays a critical role in minimizing signal reflection and maximizing coverage.

Material selection is equally important. Fiberglass, PTFE-coated fabrics, and polycarbonate are frequently used due to their structural robustness, low dielectric constant, and suitability for diverse operating environments. Factors such as temperature resistance, mechanical durability, and weight influence this choice, particularly in automotive, aerospace, or marine applications.

Ultimately, the radome is an essential component in high-frequency antenna systems, combining structural resilience with careful electromagnetic design to preserve signal integrity while adapting to environmental demands. Its integration enhances system reliability and ensures consistent radar performance across operational conditions.

4.2 Radome - Parameters

To accurately assess electromagnetic wave propagation through a radome, it is essential to understand the material's constitutive parameters—namely permittivity, permeability, and conductivity. These properties determine how electromagnetic (EM) fields

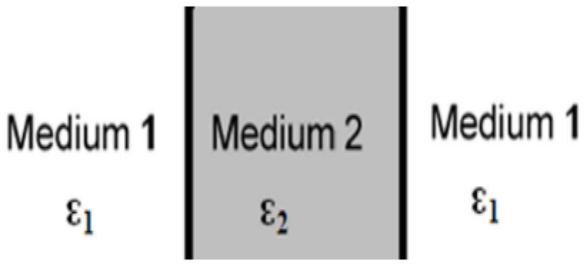

Figure 4.1: Boundary of Mismatch Between Dielectric Mediums[4]

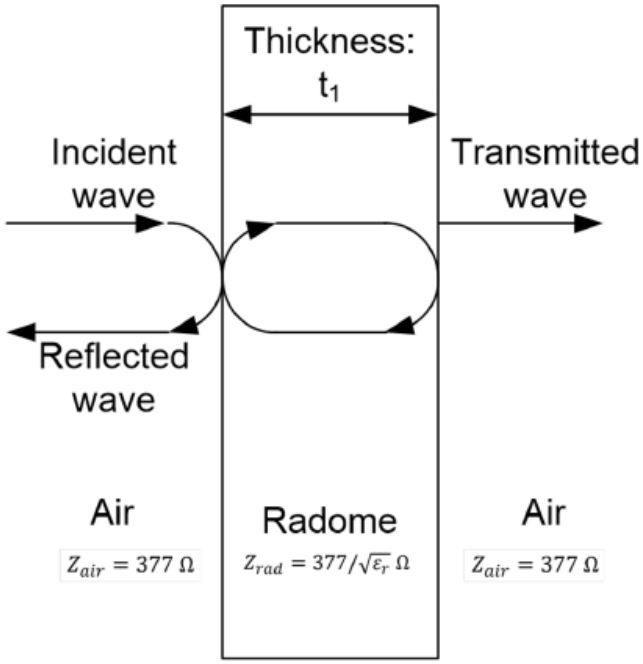

Figure 4.2: Reflections at Radome Boundaries[4]

interact with the medium. Most radomes are made from non-magnetic dielectric materials with a relative permeability of 1 and negligible electrical conductivity. A key parameter for radome design is the relative permittivity, often referred to as the dielectric constant (D_k). This governs both the refractive behavior and wave speed within the material. Since EM signals travel slower through media with higher dielectric constants compared to air, selecting a material with an optimal D_k is vital for minimizing signal distortion and preserving wavefront integrity. Signal attenuation or "fade" through a radome can occur due to two distinct reflection mechanisms. First, reflection at the air-radome boundary arises from impedance mismatch caused by differing dielectric constants, resulting in partial signal loss. Second, multiple reflections within the radome itself occur when the transmitted wave undergoes repeated internal bouncing due to material thickness or shape. These secondary reflections can introduce interference and reduce the overall transmission efficiency. To mitigate these effects, both the radome's material composition and geometry must be carefully optimized using electromagnetic simulation tools to ensure minimal reflection and maximum transparency to EM waves.

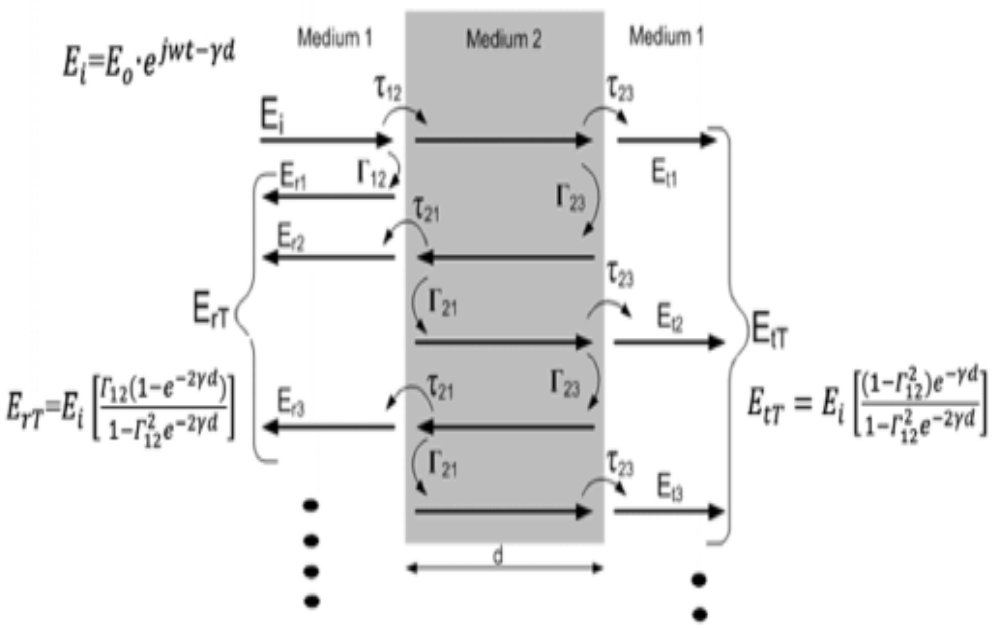

Figure 4.3: Multiple Reflections at Boundaries of Dielectric Mediums [4]

4.2.1 Radome Wall Thickness

The thickness of the radome wall plays a critical role in ensuring optimal electromagnetic transparency and overall antenna performance. To minimize reflection losses and maximize transmission, the radome thickness should be chosen as an integral multiple of half the wavelength within the material. This condition enables constructive interference and minimal attenuation. The optimum thickness is given by:

$$t_{\text{optimum}} = n \cdot \frac{\lambda_m}{2} \tag{4.1}$$

where the wavelength in the material is:

$$\lambda_m = \frac{c}{f\sqrt{\varepsilon_r}} \tag{4.2}$$

In the equations,

- t_{optimum}: Optimum radome wall thickness
- n: Integer multiplier (1, 2, 3, ...)
- λ_m: Wavelength in the radome material
- c: Speed of light
- f: Mean operating frequency (e.g., 6 GHz)
- ε_r: Relative permittivity of the radome material

4.2.2 Optimal Antenna-to-Radome Distance

The spacing between the antenna and the inner surface of the radome affects the phase alignment of reflected waves. To minimize destructive interference and preserve signal integrity, the antenna should be positioned at a distance that ensures reflected waves return in phase with the transmitted signal. This optimal distance is calculated as:

$$D = n \cdot \frac{\lambda}{2} \tag{4.3}$$

where:

- D: Optimal spacing between antenna and radome wall
- n: Integer multiplier (1, 2, 3, ...)
- λ: Wavelength in air

4.3 Flat Radome

A flat radome is a planar, electromagnetically transparent structure designed to protect antennas, especially in mmWave and microwave systems, while minimizing signal distortion. Unlike curved radomes (spherical or geodesic), flat radomes are simpler to fabricate and integrate, particularly in compact or low-profile applications.

4.3.1 Thickness of the Radome

The optimal thickness of the radome is computed using the half-wavelength criterion within the dielectric medium:

$$t_{\text{optimum}} = \frac{\lambda_m}{2} = \frac{c}{2f\sqrt{\varepsilon_r}} \tag{4.4}$$

Substituting the known values:

$$t_{\text{optimum}} = \frac{299{,}792{,}458}{2 \times 6 \times 10^9 \times \sqrt{2.8}} = 14.94\,\text{mm} \tag{4.5}$$

Thus, the optimal radome thickness is **14.94 mm**, which minimizes signal reflection and enhances electromagnetic transparency.

4.3.2 Optimal Distance Between Antenna and Radome

To reduce destructive interference from reflected waves, the ideal separation between the antenna and the inner surface of the radome is calculated by:

$$D = \frac{\lambda}{2} \tag{4.6}$$

Assuming a free-space wavelength of $\lambda = 50\,\text{mm}$:

$$D = \frac{50}{2} = 25\,\text{mm} \tag{4.7}$$

Therefore, the antenna should be positioned **25 mm** away from the internal surface of the radome to maintain constructive interference. Using the above data, a flat spherical radome is built above the patch antenna, in which the material assigned for the radome is plexiglass (Polymethyl methacrylate) PMMA is a solid candidate due to:

- Optical clarity: Transmits up to 92% of visible light, making it ideal for radomes.
- Weather-resistant: Excellent UV and environmental stability, suitable for outdoor use.
- Thermal performance: Vicat softening temperature is around 108 °C; deflection temperature ∼98 °C.
- Electrical insulation: High surface and volume resistivity, useful in RF applications
- Machinability: Can be laser-cut, thermoformed, or injection molded with precision
- Low dielectric constant (∼2.6–3.6) and low loss tangent, minimizing signal distortion.
- Mechanical strength and abrasion resistance, protecting sensitive antenna structures.
- Formability: Easily shaped into curved or complex radome geometries.

Chapter 5

Simulating the antenna with Flat radome

To accurately characterize the electromagnetic behavior of a wireless sensing setup, it is essential to simulate the integrated antenna–radome system. This simulation involves coupling a planar microstrip patch antenna with a flat dielectric radome designed for minimal signal degradation. The radome, constructed of PMMA or similar low-loss material, is modeled with defined permittivity and wall thickness based on optimal transmission criteria.

5.1 Results: Impact of the Radome on Radiation Characteristics

Simulation results reveal a measurable influence of the radome on the antenna's radiation behavior. The presence of the flat radome introduces slight beam broadening and a minor shift in the peak gain direction due to refraction at the radome-air interface. Return loss curves show minimal variation.

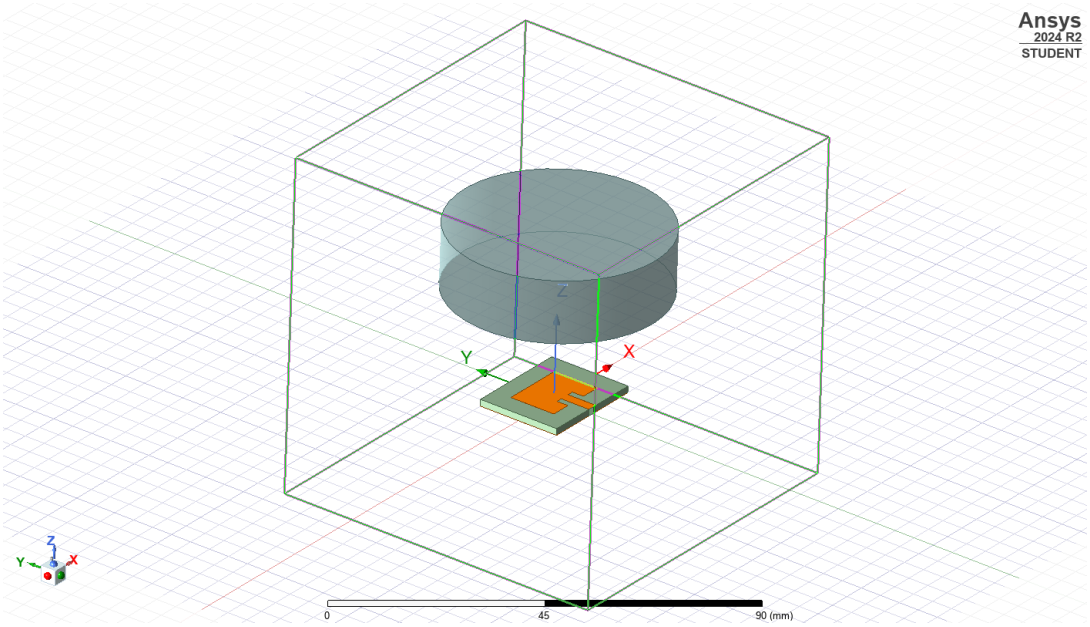

Figure 5.1: Radome CAD simulation

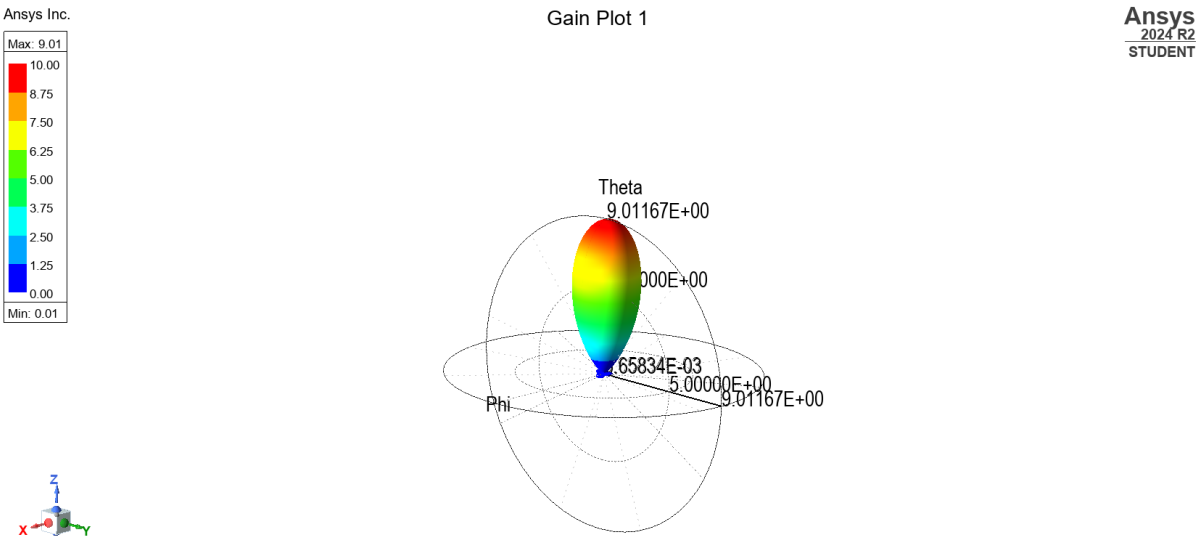

Figure 5.2: 3D polar gain plot for E and H plane with radome

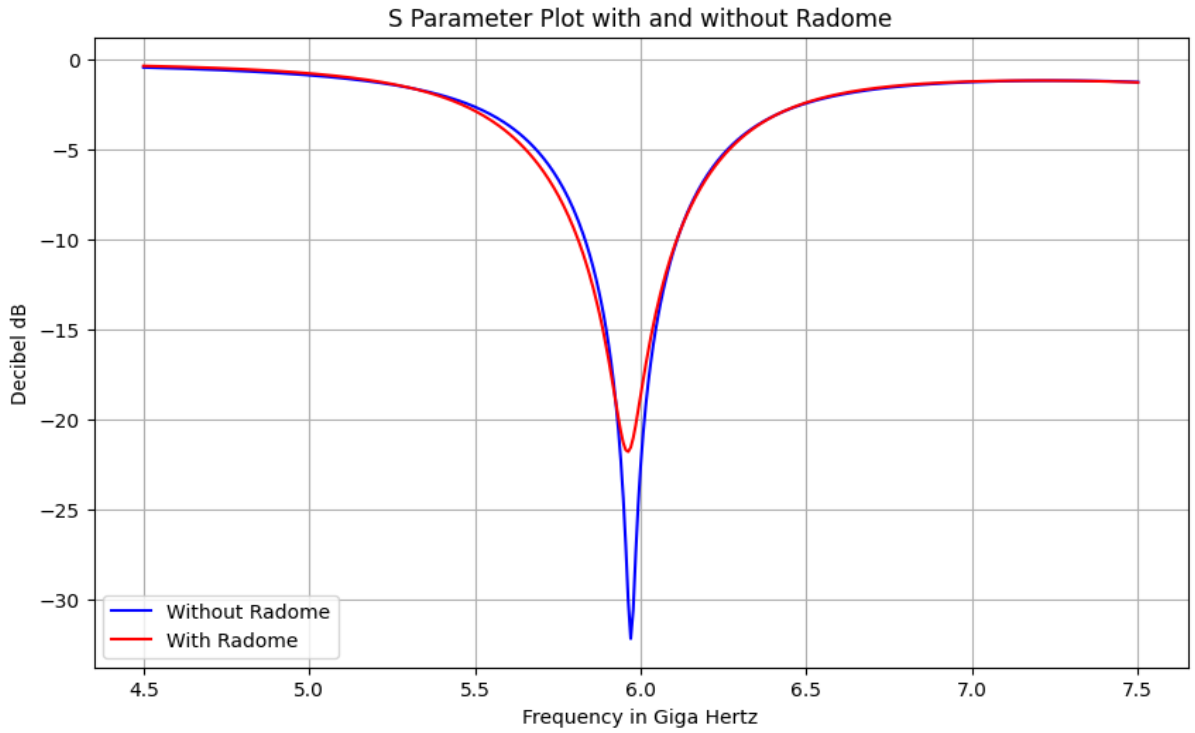

Figure 5.3: S11 parameter with and without radome

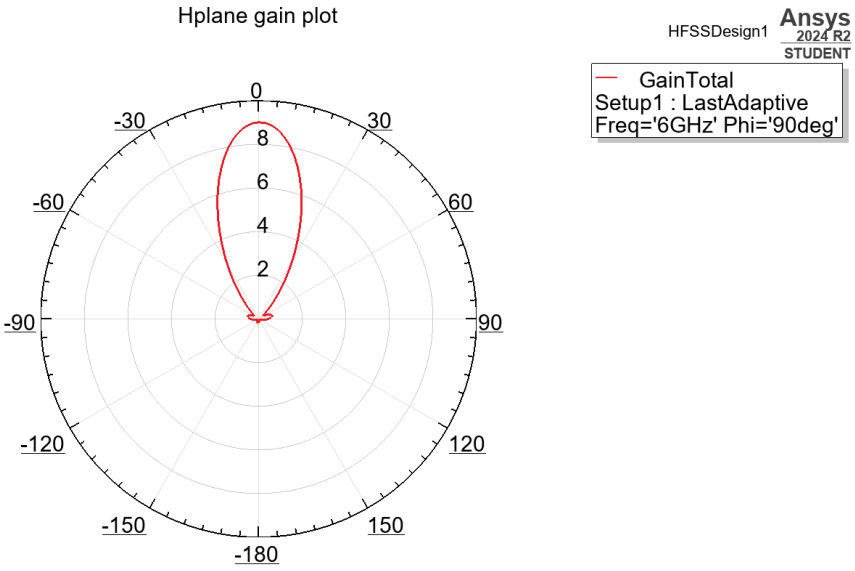

Figure 5.4: H plane 2D gain plot with radome

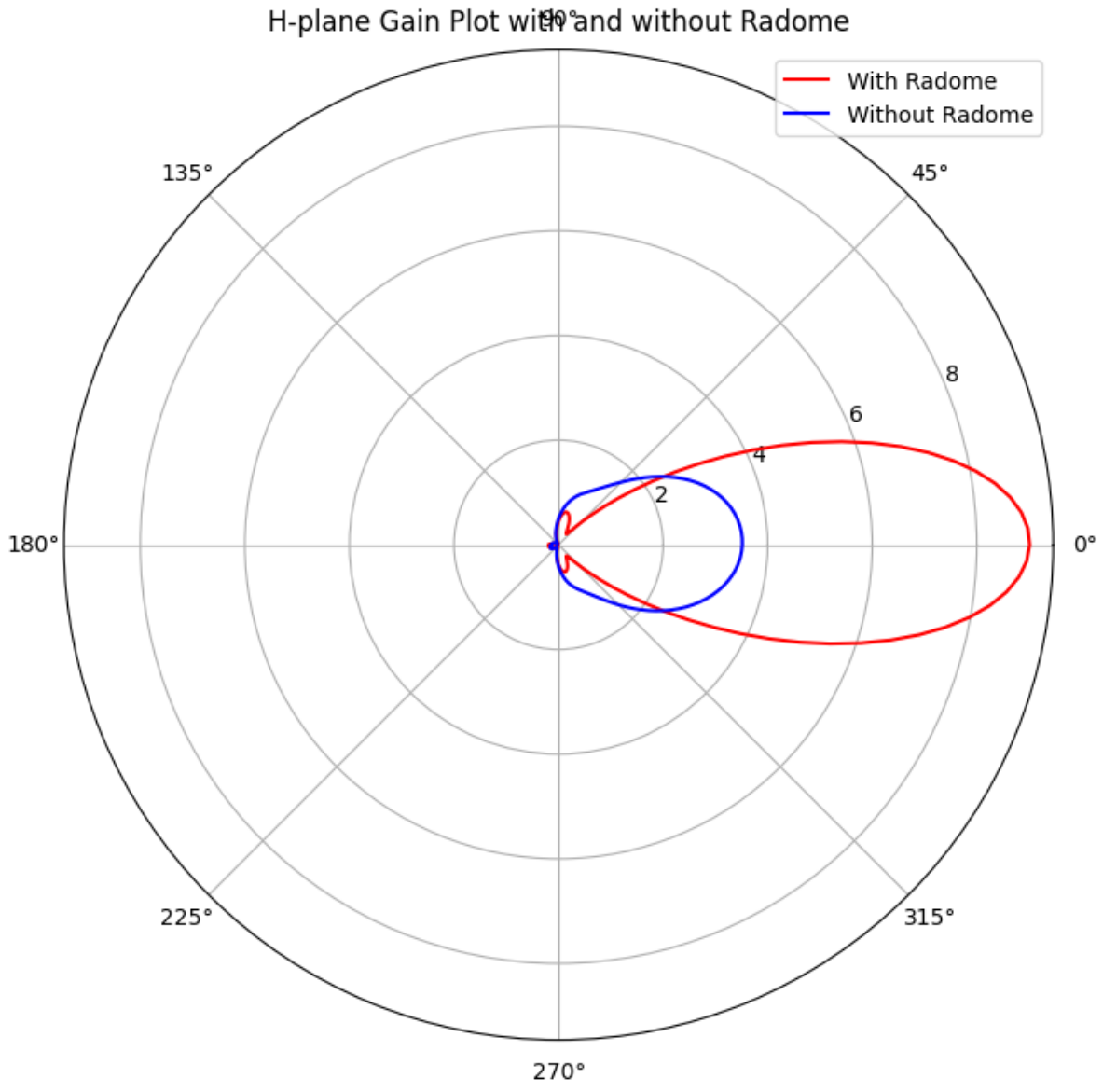

Figure 5.5: H plane 2D gain plot with radome

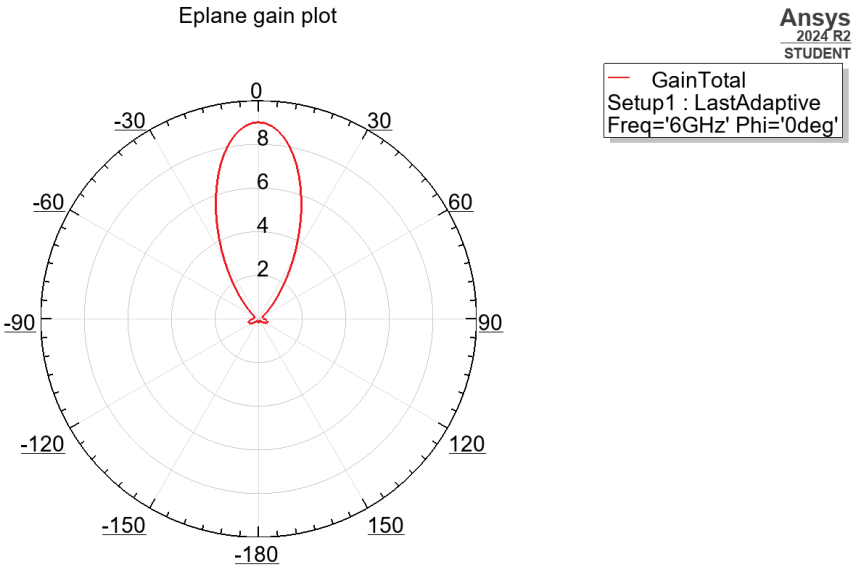

Figure 5.6: E plane 2D gain plot with radome

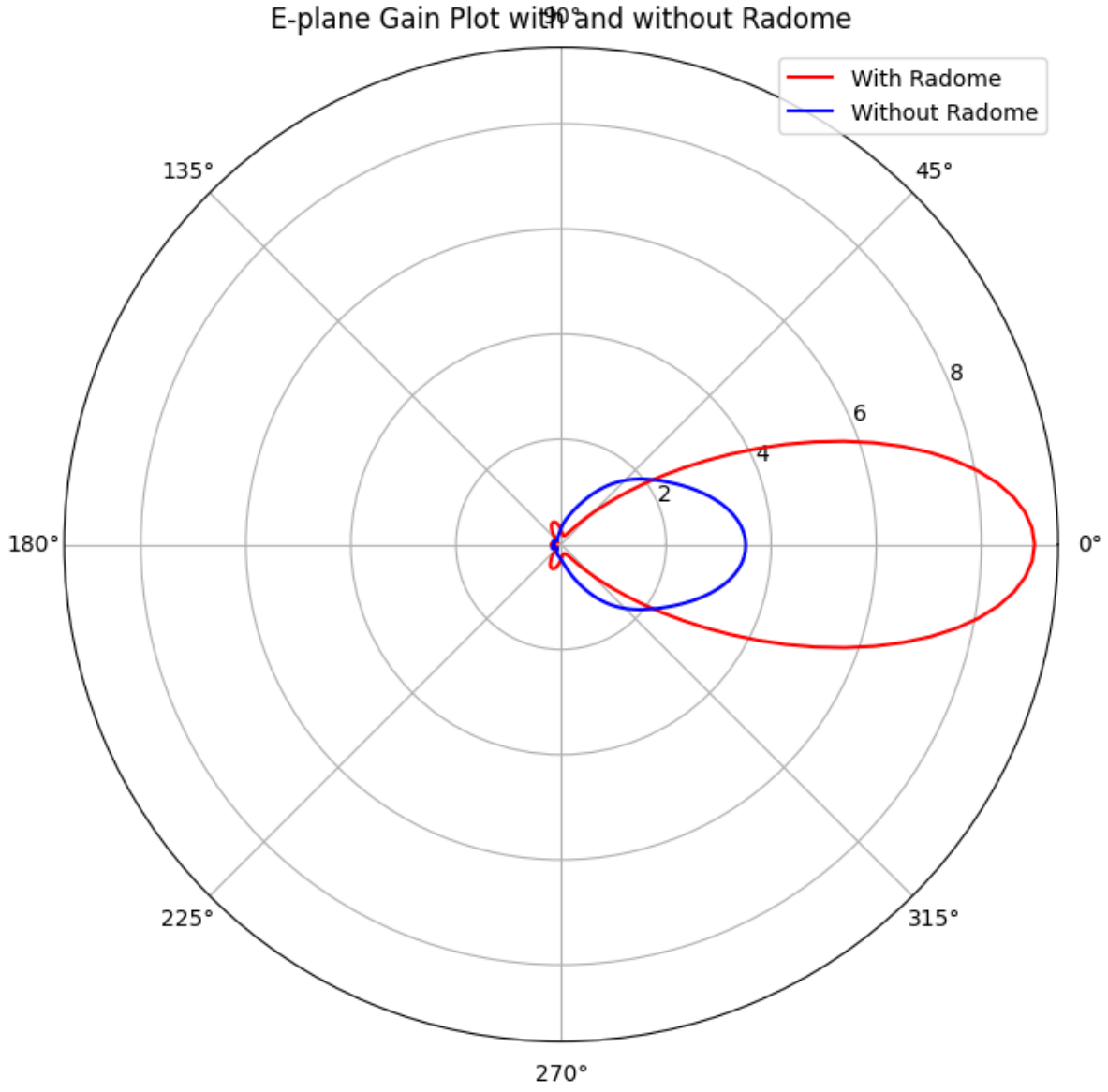

Figure 5.7: Gain plot comparison for E plane

Chapter 6

Conclusion

This thesis presents a comprehensive investigation into the performance of microstrip patch antennas with and without radome integration, emphasizing electromagnetic behavior, structural resilience, and environmental reliability. Detailed parametric simulations and comparative analyses reveal that antennas without radomes deliver marginally superior gain and cleaner radiation profiles due to the absence of dielectric interference. However, their practicality for deployment in harsh environments is limited by susceptibility to mechanical damage, moisture, and contamination.

The incorporation of radome enclosures—particularly flat A-sandwich composites—demonstrates a favorable balance between RF integrity and protective functionality. While slight increases in insertion loss (approximately 1 dB) and side lobe levels (1–2 dB) are observed, these deviations remain within acceptable tolerances when radome geometry, material properties, and joint thicknesses are carefully optimized. Minor boresight shifts and depolarization effects, particularly under wet or misaligned conditions, highlight the importance of precision in fabrication and alignment protocols.

The findings affirm that with judicious design, radome-equipped antennas offer robust solutions for outdoor and mission-critical applications without compromising essential electromagnetic performance. This study lays a foundation for extending future work toward advanced radome geometries (e.g., spherical), broader material characterization, and adaptive RF systems suited for radio astronomy, aerospace telemetry, and high-frequency remote sensing platforms.

Chapter 7

Bibliography

1. H. Werfelli *et al.*, "Design of rectangular microstrip patch antenna," in *Proc. 2nd Int. Conf. Adv. Technol. Signal Image Process. (ATSIP)*, Monastir, Tunisia, IEEE, Mar. 2016.

2. M. A. McCulloch *et al.*, "An S-band cryogenic phased array feed for radio astronomy," *RAS Techniques and Instruments*, vol. 2, no. 1, pp. 432–440, 2023.

3. I. Kazani *et al.*, "Performance Study of Screen-Printed Textile Antennas after Repeated Washing," *Autex Research Journal*, vol. 14, no. 2, pp. 47–54, 2014. https://doi.org/10.2478/v10304-012-0049-x

4. C. Kumar, H. U. R. Mohammed, and G. Peake, "mmWave Radar Radome Design Guide," Technical Report SWRA705, Texas Instruments, 2021. https://www.ti.com/lit/pdf/swra705

5. C. A. Balanis, *Antenna Theory: Analysis and Design*, 4th ed., Wiley, 2016. https://www.wiley.com/en-us/Antenna+Theory%3A+Analysis+and+Design%2C+4th+Edition-p-978